Monocyte-derived macrophages promote breast cancer bone metastasis outgrowth

Monocyte-derived macrophages promote breast cancer bone metastasis outgrowth

Ruo-Yu Ma[1], Hui Zhang[2], Xue-Feng Li[1], Cheng-Bin Zhang[1], Cigdem Selli[1], Giulia Tagliavini[3], Sandrine Prost[3], Andrew H. Sims[4], Hai-Yan Hu[5], Tianlei Ying[6], Zhan Wang[7], Zhaoming Ye[7], Jeffery Pollard[1,2]*, Bin-Zhi Qian[1,4]*,

1 MRC Centre for Reproductive Health, College of Medicine and Veterinary Medicine, Queen's Medical Research Institute, The University of Edinburgh, Edinburgh, UK;

2 Department of Developmental and Molecular Biology, Albert Einstein College of Medicine, Bronx, New York, USA.

3 MRC Centre for Inflammation Research, College of Medicine and Veterinary Medicine, Queen's Medical Research Institute, The University of Edinburgh, Edinburgh, UK;

4 Edinburgh Cancer Research UK Centre, Institute of Genetics & Molecular Medicine, University of Edinburgh, UK

5 Shanghai Jiao Tong University Affiliated Sixth People`s Hospital, Shanghai, China

6 MOE/NHC/CAMS Key Laboratory of Medical Molecular Virology, School of Basic Medical Sciences, Shanghai Medical College, Fudan University, Shanghai, China

7 Department of Orthopaedics, Centre for Orthopaedic Research, Orthopedics Research Institute of Zhejiang University, The Second Affiliated Hospital, Zhejiang University School of Medicine, Zhejiang, China

Bone metastasis is the major cause of death in breast cancer. The lack of effective treatment suggests that the underlying mechanism of bone metastasis outgrowth is still largely unknown. As a key component of tumour microenvironment, macrophages promote tumour progression and metastasis. In the current study, we found that macrophages are abundant in human and mouse breast cancer bone metastases. Macrophage ablation significantly inhibited bone metastasis growth. Lineage tracking experiments indicated that these macrophages largely derive from Ly6C+ CCR2+ inflammatory monocytes. Ablation of the chemokine receptor CCR2 significantly inhibited bone metastasis outgrowth and prolonged survival. Immunophenotyping identified that bone metastasis associated macrophages express high level of CD204 and IL4R. Furthermore, monocyte/macrophage restricted IL4R ablation significantly inhibited bone metastasis growth and IL4R-/- monocytes fail to promote bone metastasis outgrowth. Together, this study identified a subset of monocyte-derived macrophages that promote breast cancer bone metastasis in an IL4R-dependent manner. This suggests that IL4R and macrophage inhibition can have potential therapeutic benefit for breast cancer bone disease.

Introduction

Macrophages potently promote breast cancer progression and act at all steps of the metastasis cascade (Kitamura et al., 2015b; Qian and Pollard, 2010). However, these cells are heterogeneous and their phenotype and function are tightly regulated by the local tissue environment (Gordon and Pluddemann, 2019). It has become evident that most tissue resident macrophages originate from embryonic precursor cells that can persist through life. In some cases, they are replaced or complemented by bone marrow derived precursor cells, monocytes. In contrast, adult macrophages in pathophysiological situations are largely derived from monocytes (Wynn et al., 2013). Several studies, including our own, indicate that monocyte derived macrophages are critical for tumour growth and metastasis (Afik et al., 2016; Franklin et al., 2014; Lin et al., 2001; Qian et al., 2011). Tissue resident macrophages can also have an important function in tumour promotion in some cases (Zhu et al., 2017). Therefore, a better understanding of the origin and function of macrophage subsets in different cancer types and secondary organs is critical for developing precise treatment to maximize clinical benefit.

Bone metastasis is the most prevalent form of metastasis for breast cancer and accounts for over 70% of cases (Coleman, 2001). It causes bone pain, bone loss, fracture and other skeletal related events which dramatically impair patients' quality of life and causes lethality (Coleman, 2006; Weilbaecher et al., 2011). Although current therapeutic modalities such as radiotherapy, chemotherapy, and anti-osteolytic agents can reduce morbidity associated with bone metastasis, these treatments often provide minimum survival benefit to patients (Weilbaecher et al., 2011). This indicates that a better understanding of the mechanisms that lead to bone metastasis outgrowth will be critical for the development of effective treatment. Recent studies strongly argue that intricate interaction between tumour cell and supportive stroma play important roles in the development of this deadly disease(Liu et al., 2019; Price et al., 2016; Sethi et al., 2011; Wang et al., 2015; Wu et al., 2017) . For example, the osteogenic niche composed of bone-building osteoblasts has recently been shown to be critical for the survival and colonization of disseminated tumour cells (DTCs) in the bone (Shiozawa et al., 2011; Wang et al., 2015). However, the specific role of macrophage subsets in breast cancer bone metastasis is largely unknown.

In the current study, our data indicate that macrophages are critical for bone metastasis outgrowth in vivo. Combining genetic ablation models of CC chemokine receptor 2 (*Ccr2*-/-), interleukin 4 receptor (*Il4r-/-*) and a monocyte add-back approach, we have identified that a population of monocyte derived macrophage, rather than bone resident macrophages, promote breast cancer bone metastasis outgrowth in an IL4R dependent manner.

Results

Macrophage targeting inhibit bone metastasis outgrowth of breast cancer

To determine the infiltration of macrophages in patient bone metastasis samples, we stained a small cohort of patient samples (patient information see Supplemental Table 1) with CD68 as a commonly used macrophage marker. All patient samples showed significant amount of macrophage infiltration (472.8 ± 189.7 macrophages/mm^2 tumour area) (Fig 1A). Similar levels of macrophage infiltration detected by Iba1 staining is observed in a widely used in vivo model of bone metastasis using 1833 cells (a sub-line of MDA-MB-231 human triple negative breast cancer cells (Kang et al., 2003) in nude mice. This is further confirmed in bone metastasis derived from MetBo2 cells, a newly developed bone metastasis cell line derived from Polyoma middle T (PyMT) oncogene induced mouse mammary tumour in syngeneic FVB background (Fig 1B). These results confirmed that these two models represent similar level of macrophage infiltration to patient bone metastasis.

Bone metastasis outgrowth leads to macro-metastatic lesions that significantly impair patient survival and quality of life. To determine the role of macrophages in bone metastasis outgrowth, we adopted a

widely-used in vivo macrophage-ablation method of treating mice with liposome encapsulated Clodronate (L-Clod) (Qian et al., 2009; Van Rooijen and Sanders, 1994) following tumour detection in the MetBo2 and 1833 models (Fig. 1C and 1D). As expected, L-Clod treatment significantly depleted macrophages in bone metastasis without affecting other immune cell populations compared to the treatment with control liposome-PBS treatment (L-PBS) (Fig. S1A). Such macrophage ablation with L-Clod that was performed following detection of established MetBo2 cells bone lesions, significantly inhibited metastasis outgrowth in syngeneic FVB mice (Fig.1D). Colony Stimulating Factor 1 Receptor (CSF1R) is a critical lineage receptor for macrophage differentiation and function in vivo (Stanley et al., 1997). Using a specific small-molecule CSF1R inhibitor, BLZ945, we observed a significant inhibition of bone metastasis growth of MetBo2 cells in syngeneic FVB mice compared with vehicle treatment (Fig. 1E). Similarly, BLZ945 significantly inhibited bone metastasis growth of 1833 cells in nude mice (Fig. 1F). Consistent with their mode of action, BLZ945 and L-Clod, significantly reduced macrophage abundance in bone lesions without affecting other major immune cell populations (Fig S1B).

Osteoclasts, specialised cells of the macrophage lineage, have been shown to engage in paracrine signalling with cancer cells that promotes breast cancer bone disease (Maurizi and Rucci, 2018). These cells were also depleted by L-Clod treatment (Fig S2A). These data revealed that although liposomal encapsulated clodronate was originally designed to target phagocytic macrophages that actively uptake liposomes (Van Rooijen and Sanders, 1994), it also affects osteoclasts. Therefore, it is possible that part of the metastasis inhibiting effect observed in our experiments is through inhibition of osteoclasts. Soluble/free clodronate (not encapsulated in liposome) is known to target osteoclasts due to its high affinity to bone. This treatment as expected was effective (Fig S2B) and did not affect infiltration of bone metastasis associated macrophages in our models (Fig S2C). Although osteoclast inhibition with free clodronate alone can inhibitor bone metastasis growth of MetBo2 cells, the inhibition is 2.4-fold more effective with liposome clodronate that depleted both osteoclasts and bone metastasis associated macrophages (Fig S2D). Together, these data support the conclusion that bone metastasis associated macrophages can directly promote metastatic outgrowth independent of osteoclast and macrophage ablation can effectively inhibit bone metastasis outgrowth in vivo.

CCL2 recruited inflammatory monocyte promote bone metastasis growth

Macrophages in most tissues can be derived from both bone marrow monocyte precursor cells and from tissue resident macrophages originated from yolk sac precursor cells (Cassetta and Pollard, 2018; Schulz et al., 2012). Tissue resident macrophages have been shown to promote tumour progression with a pro-fibrotic phenotype in pancreatic cancer models (Zhu et al., 2017). Bone marrow resident macrophages express CD169 as a cell surface marker (Batoon et al., 2017; Hashimoto et al., 2013) . In our model, CD169+ macrophages were mainly associated with tumour adjacent stroma (Fig. S3A). These CD169+ macrophages can be efficiently depleted in transgenic mice expressing diphtheria toxin receptor under the control of CD169 promoter (CD169-DTR) upon diphtheria toxin (DT) treatment (Fig. S2B and C) which led to a significant reduction of total macrophage numbers (Fig. S3B) compared with the control treatment with a mutant toxin (Glu-DT) that because of a point mutation does not bind to theDT receptor. This ablation did not affect bone metastasis growth (Fig. S3C). Immunofluorescent staining showed a significant ablation of CD169+ macrophages without affecting the majority of tumour infiltrating macrophages labelled by lineage marker Iba1 (Fig. S3D). This indicates that bone resident macrophages do not play a major role in our model and strongly suggest that tumour promoting BoMAMs were mainly derived from recruited monocytes.

Monocytes are heterogeneous and the two most well characterized populations in mice are Ly6C expressing inflammatory monocytes (IMs; classical monocytes) and patrolling monocytes (PMs; non-classical or resident monocytes) lacking Ly6c (Auffray et al., 2009; Geissmann et al., 2010). To understand the origin of BoMAMs, we measured monocyte recruitment following adoptive transfer of each sub-set. Mouse monocytes were identified by their expression of CD11b and CD115 and were

FACS sorted into IM and RM based on Ly6C expression. As previously reported, both populations have similar level of GFP expression in *Csf1r*–GFP transgenic mice (Qian et al., 2011). We adoptively transferred 10^5 cells of each population into syngeneic FVB mice bearing bone metastasis of MetBo2 cells or healthy mice as controls (Fig. 2A). Eighteen hours after adoptive transfer, we determined the number of GFP-positive monocytes in the bone to measure their relative recruitment. Our previous studies have shown that at this time point similar numbers of donor cells were present in the blood showing equivalent availability (Qian et al., 2011). In healthy bone morrow, these two populations were recruited to a comparable level. However, in bone metastases, inflammatory monocytes were preferentially recruited, with about 2-fold enrichment (Fig. 2B).

CC chemokine ligand 2 (CCL2) and CC chemokine receptor 2 (CCR2) signalling is the major chemoattractant that mediate the recruitment of Ly6C+ inflammatory monocytes (Getts et al., 2008; Palframan et al., 2001). Consistent with a previous report (Shi et al., 2011), circulating inflammatory monocytes were significantly reduced in *Ccr2-/-* mice compared with their littermates (Fig S4A) but not in the bone marrow (Fig S4B). The bone colonization efficiency of MetBo2 cells was significantly inhibited in *Ccr2-/-* mice leading to reduced growth and prolonged survival compared with wild type controls (Fig. 2C and 2D). Consistent with these data, bone colonization efficiency of 1833 cells were also significantly inhibited in mice with CCR2 knockout compared with wild type controls (Fig. 2E and F). Furthermore, CCL2 blockade using neutralizing antibody 48 hours after tumour cell inoculation significantly inhibited 1833 bone metastasis growth (Figure 2G). Since our previous studies indicate that tumour cell metastatic extravasation and seeding mostly occur within 36 hours after reaching distal organ, these data strongly suggest that recruitment of inflammatory monocyte is critical for tumour metastatic outgrowth after seeding. To further test this, we established bone metastasis of MetBo2 cells in *Ccr2-/-* mice that have deficiency in circulating monocytes and delayed tumour growth. Upon bone metastasis detection, add-back of wild type IMs via adoptively transfer, significantly promoted tumour outgrowth compared with *Ccr2-/-* monocytes (Fig. 2H). Together these data indicate that CCL2/CCR2 dependent recruitment of IM is critical for breast cancer bone metastasis outgrowth.

Bone metastasis associated macrophages bear distinct cell surface markers

To further characterize bone metastasis associated macrophages, we performed gene expression profiling of macrophages isolated from bone metastasis and identified 409 up-regulated genes and 527 down-regulated genes compared with macrophages from healthy bone with the threshold of 1.5-fold change and $p<0.01$ (Fig 3A). For major macrophage polarisation marker genes, macrophages associated with bone metastasis express higher level of some alternative activation markers (e.g. *Il4ra, Il10*), but also some of the classical activation markers (e.g. *Tnf, Il1b*) (Fig. 3B) compared with their counterpart from healthy bone. Further analysis indicated upregulation of genes related to several tumour promoting functions related to angiogenesis, tumour growth, cancer stem cells, immune suppression etc., in BoMAMs compared with normal counterpart (Fig 3C). These are consistent with previous reported tumour promotion function of macrophages in other contexts (Cassetta et al., 2019; Ojalvo et al., 2009; Yang et al., 2018). Immunophenotyping of macrophages (defined by CD45+CD11b+F4/80+Ly6C-Ly6G-SSC^{lo}) (Chow et al., 2011) isolated from bone metastasis of MetBo2 cells, adjacent normal tissue and compared with their counterparts from normal bone using a set of macrophage polarization markers, including CD204, CD206, CD86, CD64, MHCII, and IL4R, indicated that all three macrophage populations have heterogeneous expression of these markers (Fig. 3D). Bone metastasis associated macrophages have higher IL4R expression and increased abundance of CD204+ cells (Fig. 3D). Multi-parameter FACS analysis indicated that IL4R and CD204 co-localize and label a distinct population of macrophages that are specific for bone metastasis (Fig. 3E). Immunofluorescent staining further confirmed that CD204 staining specifically labelled macrophages that infiltrate inside bone metastasis, which have relatively low F4/80 expression compared with the macrophages in adjacent normal bone marrow (peri-tumour) (Figure 3F). Consistently, these CD204+

macrophages co-express IL4R and lineage marker Iba1 as assessed by double immunofluorescent staining (Figure 3G). Importantly, in patient bone metastases samples, CD204 positive macrophages infiltrated in the tumour in all the cases in our cohort and majority of these macrophages also express IL4R (Fig. 4A). Furthermore, in two independent breast cancer bone metastasis dataset, CD204 expression is strongly correlated with macrophage IL-4R target gene score (Palazon et al., 2017; Zhang et al., 2009) (Fig. 4B). Together, these data strongly suggest IL4R signalling in macrophages plays an important role in breast cancer bone metastasis.

Monocyte derived macrophage promotion of bone metastasis is IL4R dependent

Ly6C+ CCR2+ monocytes are mostly CD204+ in both healthy or bone metastasis bearing mice (Fig. 5A) and bone metastasis associated monocytes have significant higher IL4R expression compared with normal counterparts in gene expression profile analysis (Fig. 5B). Since our data indicate that Ly6C+ inflammatory monocyte recruitment is enhanced in bone metastasis (Fig. 2B), we hypothesized that CD204+IL4R+ BoMAMs are mainly derived from inflammatory monocytes. To test this directly, we performed lineage tracing experiment using adoptive transfer of Ly6C+ monocytes FACS sorted from ubiquitous GFP expressing mice (FVB.Cg-Tg(CAG-EGFP)B5Nagy/J) into syngeneic mice bearing established bone metastasis and recovered GFP+ cells for immunophenotyping (Fig. 5C Left). Compared with endogenous macrophages (GFP-), monocyte derived macrophages (GFP+) almost exclusively express both CD204 and IL4R and represent tumour infiltrating BoMAMs while the endogenous macrophages (GFP-) are largely IL4R- and have dichotomized expression of CD204 (consistent with data in Fig. 3A) (Fig. 5C). These data directly indicate that the majority of IL4R+ bone metastasis associated macrophages are derived from recruited inflammatory monocytes.

IL4R has been shown to have multiple functions in different cell types including macrophages, T and B lymphocytes and non-hematopoietic cells (Ho and Miaw, 2016). To test the role of macrophage IL4R in bone metastasis, we crossed *Il4ra*-/- mice (Mohrs et al., 1999) with *Rag2*-/- mice that lack mature T and B cells. These mice were then used as bone marrow donors to generate mosaic mice in lethally irradiated *Foxn1* nude mice. As a result, these mosaic mice lack mature T and B function and the IL4R deficiency is limited to bone marrow derived innate immune cells, predominantly macrophages. Bone colonization potential of 1833 cells was significantly inhibited in mosaic mice bearing *Il4ra*-/- bone marrow compared with control mosaic mice containing *Il4ra*+/- bone marrow (Fig. 5D). Furthermore, osteoclast abundance in IL4R-/- bone marrow mosaic mice was comparable with that in control mice with *Il4ra*+/- bone marrow (Fig. S5A). In contrast, abundance of CD204+ BoMAMs was significantly reduced (Fig. S5B). This suggests that IL4R is important for activation of BoMAMs but not osteoclasts.

Additional experiments were performed to determine *Il4* mRNA expression using quantitative PCR on various cell types purified from the bone metastasis environment by FACS sorting. Our data indicate that CD4+ T cells have the highest *Il4* expression, tumour cells and B cells also have some *Il4* mRNA expression while all other cell type tested did not have detectable *Il4* expression. (Fig S5C).This suggests a paracrine signalling between CD4+ T cells and BoMAMs through IL-4 which is consistent with previous studies in primary breast cancer models (DeNardo et al., 2009).

Our data indicate that BoMAMs are derived from Ly6C+ IMs. The abundance of monocytes and macrophages in *Il4ra*-/- bone marrow mosaic mice are similar to *Il4ra*+/- control with comparable bone metastasis burden (Fig. S5B). This suggest that IL4R mainly affects BoMAM tumour promoting function rather than their recruitment. Indeed, in similar monocyte add back experiment as described in Fig. 2H, IL4R-/- monocytes are less efficient in promoting bone metastasis growth compared with IL4R+/+ monocytes despite equivalent recruitment (Fig. 4F). Together, these data show that stromal and tumour IL4 induced macrophage IL4R signalling is critical for BoMAM activation and their tumour promoting function.

Discussion

Compelling evidence indicate that macrophages play important roles in cancer metastatic progression and that targeting macrophage can have significant therapeutic benefit (Cassetta and Pollard, 2018; Quail and Joyce, 2016; Ruffell and Coussens, 2015) Nevertheless, metastasis still remains a major cause of death. In particular, in breast and other cancers outgrowth of bone metastasis represent a major clinical challenge (Mundy, 2002). The current study provides direct evidence that macrophages are critical for breast cancer bone outgrowth. Macrophage ablation or inhibition of CSF1 receptor potently inhibited bone metastasis outgrowth of both murine and human breast cancer cells in immune competent and immune deficient mice respectively. These data suggest that macrophage targeting might be an effective therapeutic approach in treating breast cancer bone disease.

Macrophages can be derived at least from embryonic precursor cells and bone marrow monocytes (Jacome-Galarza et al., 2019). In the current study, our data strongly suggest that monocyte derived BoMAMs are critical for bone metastasis outgrowth in an IL4R dependent manner. BoMAMs express low levels of F4/80 in immunofluorescent staining, which is one of the characteristics of monocyte derived macrophages (Schulz et al., 2012). Consistent with this data, a deficiency in CCR2-dependent monocyte recruitment significantly inhibited bone colonization efficiency whilst addback of wild type monocytes restored bone metastasis outgrowth. Embryonic precursor cells give rise to tissue resident macrophages in almost all tissues (Perdiguero and Geissmann, 2016). Studies by Frenette's group and others, suggest that CD169+ macrophage represent bone resident macrophages that control the peri-vascular hematopoietic stem cell niche (Chow et al., 2013). In the current study, depletion of these macrophages using CD169-DTR mice did not affect metastasis outgrowth. Consistent with this result, we found that majority of the resident macrophages do not express IL4R a receptor that is critical for bone metastasis outgrowth. Together with the data from *Ccr2-/-* mice and the monocyte add-back rescue experiments, this indicate that, at least in the models tested here, bone metastasis promoting macrophages are predominantly derived from recruited inflammatory monocytes. Interestingly the contribution of tissue resident macrophages can vary among different secondary organs and cancer types. For example, resident macrophages have been shown to play an important role in tumour progression of primary pancreatic adenocarcinomas (Zhu et al., 2017). Therefore, distinct macrophage subsets may play dominant roles in different cancer types and in different secondary organs. This suggests the need for precisely targeted therapies to maximize patient benefits.

It is interesting that adoptive transfer of wild type inflammatory monocyte, but not *Ccr2-/-* counterpart, can significantly promote bone metastasis growth in *Ccr2-/-* mice. These data suggest that CCR2 dependent monocyte recruitment is critical for bone metastasis outgrowth. Our previous studies showed a similar mechanism of monocyte in promotion of breast cancer lung metastasis seeding and extravasation (Qian et al., 2011). In both cases, tissue resident macrophages did not seem to play major tumour supporting roles. Interestingly, Kuffer cell and microglia, tissue resident macrophage of liver and brain respectively, have been shown to play important roles in the process of breast cancer metastasis to these two target organs (Bowman et al., 2016; Gordon et al., 2017; Hoshino et al., 2015; Zhu et al., 2017). Together these data underline macrophage heterogeneity as an important component of tissue microenvironment (the 'soil') that determines tissue specific metastasis mechanisms. Of note, CCL2/CCR2 axis may also regulate the phenotype(Sierra-Filardi et al., 2014) or function of macrophages as have been shown in melanoma, lung and liver cancer models (Kitamura et al., 2015a; Li et al., 2017; Xu et al., 2019). Our data cannot exclude the possibility that similar mechanism may also exist in breast cancer bone metastasis following the recruitment of inflammatory monocytes.

IL4R have been shown to induce alternative activation of macrophages (Varin et al., 2010), Ig production in B cells (Yanagihara et al., 1995), activation of type 2 T helper cells as well as signalling in non-hematopoietic cells (Li et al., 2009). Previous studies have illustrated the role of IL4/IL4R signalling in tumour invasion and response to treatment in primary breast cancer models (Andreu et al., 2010; Venmar et al., 2014) and glioma models (Pyonteck et al., 2013). The current study revealed that IL4R signalling is critical for the polarisation and pro-tumour function of bone metastasis associated macrophages. Together, these data suggest that IL4/IL4R pathway can be a promising target in neutralizing tumour promoting macrophages.

In summary, here we have elucidated a novel mechanism that promotes breast cancer bone metastasis outgrowth through a specific subset of CD204+IL4R+ macrophages derived from CCR2 recruited inflammatory monocyte. This population of bone metastasis associated macrophage is preserved in patient bone metastasis samples. This mechanism can be potentially targeted to treat breast cancer bone disease.

Material and Methods

Animal studies. All animal procedures were performed based on the United Kingdom Animals Act 1986 following the local rules and approved project licence or in accordance with National Institutes of Health regulations concerning the use and care of experimental animals with approval by the Albert Einstein College of Medicine Animal Use Committee. FVB/N, athymic Nude (Outbreed, mixed background) and albino-b6 was bought from Charles River. B6.129S4-Ccr2tm1Ifc/J (*Ccr2*$^{-/-}$) mice, B6.Il4ratm1Sz/J(*Il4ra*-/-) mice, B6(Cg)-Rag2tm1.1Cgn/J(*Rag2*-/-) and FVB.Cg-Tg(CAG-EGFP)B5Nagy/J (FVB-eGFP) mice were bought from Jackson Laboratory. CD169-DTR mice were acquired from Albert Einstein College of Medicine, USA. *Csf1r-EGFP* (MacGreen) mice on the C57BL/6 background were obtained from Dr David Hume (University of Edinburgh, UK). *Ccr2*-/- mice and CD169-DTR mice were crossed with athymic mice. *Il4ra*-/- mice were crossed with *Rag2*-/- mice. For generation of bone marrow mosaic mice, recipient mice receive 8Gy irradiation at the age of 3 weeks and rested for 5 hours before intravenously inject of bone marrow cells from donor mice. The mice were recovered for 3 weeks before performing metastasis assays. All the in vivo experiments were repeated at least twice with over 3 mice in each group.

Human tissue and multiplex immunofluorescent staining. The Bone metastases samples were collected from 9 patients diagnosed with grade IV breast cancer from 2016 to 2017. This study followed standard guidelines and was approved by the Ethics Committee of the Second Affiliated Hospital of Zhejiang University School of Medicine, Hangzhou, China. Multiplex staining was performed with slides cut from formalin-fixed and paraffin-embedded patient bone metastasis samples. Their demographic information, including gender, sampling site and molecular phenotype was shown in Table S1. For PanCK staining, slides were retrieved in 0.125mM EDTA solution (pH=8.0) at 97°C for 45 minutes in pressure cooker. After cooling down, samples were incubated in 30% hydrogen peroxide for 30 minutes and blocked. The staining was performed using Alexa Fluor™ 488 Tyramide SuperBoost™ Kit (ThermoFisher, US, B40941) via protocol recommended by the antibody providers. For multiplexing staining, we used the method described previously (Prost et al., 2016) and the protocols provided by manufactures. Anti-human primary antibodies used: PanCK (AE1/AE3, ThermoFish), CD204 (SRA-E5, Abnova), CD68 (PG-M1, Dako), IL-4Ra (MAB230, R&D). Other products used: serum free block (DAKO, US, X0909), Qred (1/750, ThermoFisher, US, Q10363). Avidin/Biotin blocking kit (Vector, US, SP-2001), EcoMount (Biocare Medical, UK, EM897L). Sample were scanned and unmixed using Polaris multispectral slide scanner (Vectra) and analysed using Nuance.

Mouse bone metastasis samples were fixed by 4% PFA for 30 minutes, incubated with 30% sucrose overnight then embedded in OCT at -20°C. Then bone was shaved to expose bone marrow and washed in PBS and blocked with 5% BSA and anti-mouse CD16/32 antibody (BD Biosciences, 1:200). Primary antibodies and secondary antibodies were stained in dark. Bone was imaged under spinning disk confocal microscope. 3D images were generated via Volocity. FACS antibodies as described below and Anti-Iba1 (WDR2342) were used for staining.

Cell culture. MetBo2 is a selected bone homing clone of murine breast cancer cell line Met-1, which derived from Polyoma Middle T Oncoprotein (PyMT) tumour previously (Qian et al., 2009). Human breast cancer cell line 1833 (bone metastatic clone of triple negative breast cancer cell line MDA-MB-231, gift from Prof Joan Massagué). Cells were cultured in Dulbecco's Modified Eagle Medium (DMEM, Gibco) supplemented with 10% heat-inactivated fetal bovine serum (FBS) (Gibco) and 1% v/v penicillin-streptomycin (P/S) (Gibco). Cells were maintained at 37°C with 5% v/v CO_2 in incubator. All cells were negative for mycoplasma (ABM). STR test were performed for human cells to make sure of their purity.

Experimental metastasis assay and treatment. Bone metastasis was generated through intra-cardiac injection of $1x10^5$ tumour cells into 4-week-old female mice of respective strains described above. Bioluminescent signal was recorded twice a week use Photon IMAGER Optima system (Biospace) or IVIS spectrum (PerkinElmer). The region of interest was quantified by Photon IMAGER™ software or IVIS Living Imaging 4.3.1. Macrophage depletion was performed by intravenous injection of liposome clodronate (Liposoma) (1mg/mice) twice a week. BLZ945 was given as daily gavage (200mg/kg body weight). CCL2-neutralizing antibody or the control antibody (Ortho BiotechOncology) were treated (20mg/kg body weight) twice a week.

For adoptive transfer, 1 $x10^6$ monocytes (CD45+CD11b+CSF1R$^+$Ly6C$^+$) from wild-type, *Ccr2*$^{-/-}$ or *Il4ra*$^{-/-}$ were sorted and injected via intra-caudal injection to mice with detecable bone metastasis. Mice were imaged right before monocyte transfer, and day 0, 1, 3,7 and 10 for quantification of tumour growth. For lineage tracking, 1 $x10^6$ GFP+ monocytes (from FVB-eGFP or *Csf1r-EGFP* mice) were injected intravenously into mice with late-stage bone metastasis. Bone and blood were collected 48hr after injection.

FACS analysis. For mice with bone metastasis, bone was separated into tumour and peri-tumour areas based on the bioluminescent signal. Samples were then digested in DMEM supplemented with Librease TL, Librease DL, DNAase I and Hyaluronidase (1:100 each) on shaker at 37°C for 30 minutes. Blood was drawn by cardiac puncture with heparin (Sigma-Al). Spleen was mashed using the plunger from an insulin syringe into a 40uM cell strainer (Falcon). Red blood cell lysis buffer (eBioscience) was used to remove red blood cells. Cells were blocked with anti-mouse CD16/32 antibody (BD Biosciences, 1: 500) before staining. Surface markers were stained for 30 minutes on ice and washed by PBS. Cells were sorted on Aria II or Fusion, or analysed on Fortessa (BD Bioscience). Antibodies used are the following: CD11b (M1/70), Ly6G (1A8), Ly6C (HK1.4), F4/80 (BM8), CCR2 (FAB5538A), CD45 (30-F11), CD64(X54-5/7.1), CD86 (GL-1), CD115 (AFS98), CD169 (SER-4), CD206 (C068C2), MHCII (M5/114.15.2), MSR-1 (FAB1797P), Mouse IgG1 (MOPC-21), Rat IgG2a (RTK2758), Hamster IgG (HTK888), B220 (RA3-6B2), CD3 (17A2), CD4 (RM4-5), CD8a (53-6.7), CD19 (6D5), NK1.1(PK136).

FACS sorting and gene expression array analysis. Tissue preparation and antibodies were same as described in FACS analysis. Inflammatory monocytes (Ly6C+) were sorted from bones bearing metBo2 or 1833 bone metastasis or healthy controls. Total RNA was extracted from these sorted macrophages (RNeasy Mini kit; QIAGEN), and its quality was determined using Pico Chip with a 2100 Bioanalyzer (Agilent Technologies). Samples where then submitted to Einstein microarray facility for labeling and

hybridization on Aymetrix MoGene 2.0 st chips. Differential gene expression analysis was performed using R and limma (Ritchie et al., 2015). Genes with log2FC > ±1.5 and P<0.05 were considered differentially expressed.

Bioinformatics. Bioinformatics analysis was performed with R and Bioconductor. Gene annotation was performed using database of The Database for Annotation, Visualization and Integrated Discovery (DAVID). For survival analysis, a publicly available dataset (n=368), which is a combination of MSK82 [GSE2603] and EMC286 [GSE2034] with bone only-metastasis free and other (brain and lung) metastasis-free survival information was used. Patients were stratified based on pathological ER status (113 ER-negative, 255 ER-positive) and IL4R expression. Significance and hazard ratio values were calculated for all possible separation points (cut-off) of IL4R expression using survivALL package(Pearce et al., 2018). Cox proportional-hazards model was used to calculate P and HR values (Therneau and Grambsch, 2000). For correlation analysis, three individual datasets with breast cancer bone metastasis samples (GSE14020 and GSE54323) were used. IL4 target score was calculated using differentially regulated genes in IL4-treated macrophages reported by Gupta et.al. (Gupta et al., 2018) and Single-sample Gene Set Enrichment Analysis(Barbie et al., 2009) and GSVA package (Hänzelmann et al., 2013). Pearson correlation analysis was used to analyse the correlation between IL4 target scores and IL4R and CD204 expression.

Statistical analysis. Statistical analysis was performed with GraphPad Prism (Version 7). Two-tailed student t test and ANOVA followed by multiple comparison was used to calculate statistical significance. The difference was considered as significant with a p-value lower than 0.05.

References:

Afik, R., E. Zigmond, M. Vugman, M. Klepfish, E. Shimshoni, M. Pasmanik-Chor, A. Shenoy, E. Bassat, Z. Halpern, T. Geiger, I. Sagi, and C. Varol. 2016. Tumor macrophages are pivotal constructors of tumor collagenous matrix. *The Journal of experimental medicine* 213:2315-2331.

Andreu, P., M. Johansson, N.I. Affara, F. Pucci, T. Tan, S. Junankar, L. Korets, J. Lam, D. Tawfik, D.G. DeNardo, L. Naldini, K.E. de Visser, M. De Palma, and L.M. Coussens. 2010. FcRgamma activation regulates inflammation-associated squamous carcinogenesis. *Cancer cell* 17:121-134.

Auffray, C., M.H. Sieweke, and F. Geissmann. 2009. Blood monocytes: development, heterogeneity, and relationship with dendritic cells. *Annual review of immunology* 27:669-692.

Barbie, D.A., P. Tamayo, J.S. Boehm, S.Y. Kim, S.E. Moody, I.F. Dunn, A.C. Schinzel, P. Sandy, E. Meylan, C. Scholl, S. Frohling, E.M. Chan, M.L. Sos, K. Michel, C. Mermel, S.J. Silver, B.A. Weir, J.H. Reiling, Q. Sheng, P.B. Gupta, R.C. Wadlow, H. Le, S. Hoersch, B.S. Wittner, S. Ramaswamy, D.M. Livingston, D.M. Sabatini, M. Meyerson, R.K. Thomas, E.S. Lander, J.P. Mesirov, D.E. Root, D.G. Gilliland, T. Jacks, and W.C. Hahn. 2009. Systematic RNA interference reveals that oncogenic KRAS-driven cancers require TBK1. *Nature* 462:108-112.

Batoon, L., S.M. Millard, M.E. Wullschleger, C. Preda, A.C. Wu, S. Kaur, H.W. Tseng, D.A. Hume, J.P. Levesque, L.J. Raggatt, and A.R. Pettit. 2017. CD169(+) macrophages are critical for osteoblast maintenance and promote intramembranous and endochondral ossification during bone repair. *Biomaterials*

Bowman, R.L., F. Klemm, L. Akkari, S.M. Pyonteck, L. Sevenich, D.F. Quail, S. Dhara, K. Simpson, E.E. Gardner, C.A. Iacobuzio-Donahue, C.W. Brennan, V. Tabar, P.H. Gutin, and J.A. Joyce. 2016. Macrophage Ontogeny Underlies Differences in Tumor-Specific Education in Brain Malignancies. *Cell Rep* 17:2445-2459.

Cassetta, L., S. Fragkogianni, A.H. Sims, A. Swierczak, L.M. Forrester, H. Zhang, D.Y.H. Soong, T. Cotechini, P. Anur, E.Y. Lin, A. Fidanza, M. Lopez-Yrigoyen, M.R. Millar, A. Urman, Z. Ai, P.T. Spellman, E.S. Hwang, J.M. Dixon, L. Wiechmann, L.M. Coussens, H.O. Smith, and J.W. Pollard. 2019. Human Tumor-Associated Macrophage and Monocyte Transcriptional Landscapes Reveal Cancer-Specific Reprogramming, Biomarkers, and Therapeutic Targets. *Cancer cell* 35:588-602 e510.

Cassetta, L., and J.W. Pollard. 2018. Targeting macrophages: therapeutic approaches in cancer. *Nature reviews. Drug discovery* 17:887-904.

Chow, A., M. Huggins, J. Ahmed, D. Hashimoto, D. Lucas, Y. Kunisaki, S. Pinho, M. Leboeuf, C. Noizat, N. van Rooijen, M. Tanaka, Z.J. Zhao, A. Bergman, M. Merad, and P.S. Frenette. 2013. CD169+ macrophages provide a niche promoting erythropoiesis under homeostasis, myeloablation and in JAK2V617F-induced polycythemia vera. *Nature medicine* 19:429-436.

Chow, A., D. Lucas, A. Hidalgo, S. Mendez-Ferrer, D. Hashimoto, C. Scheiermann, M. Battista, M. Leboeuf, C. Prophete, N. van Rooijen, M. Tanaka, M. Merad, and P.S. Frenette. 2011. Bone marrow CD169+ macrophages promote the retention of hematopoietic stem and progenitor cells in the mesenchymal stem cell niche. *The Journal of experimental medicine* 208:261-271.

Coleman, R.E. 2001. Metastatic bone disease: clinical features, pathophysiology and treatment strategies. *Cancer treatment reviews* 27:165-176.

Coleman, R.E. 2006. Clinical features of metastatic bone disease and risk of skeletal morbidity. *Clinical cancer research : an official journal of the American Association for Cancer Research* 12:6243s-6249s.

DeNardo, D.G., J.B. Barreto, P. Andreu, L. Vasquez, D. Tawfik, N. Kolhatkar, and L.M. Coussens. 2009. CD4(+) T cells regulate pulmonary metastasis of mammary carcinomas by enhancing protumor properties of macrophages. *Cancer cell* 16:91-102.

Franklin, R.A., W. Liao, A. Sarkar, M.V. Kim, M.R. Bivona, K. Liu, E.G. Pamer, and M.O. Li. 2014. The cellular and molecular origin of tumor-associated macrophages. *Science* 344:921-925.

Geissmann, F., M.G. Manz, S. Jung, M.H. Sieweke, M. Merad, and K. Ley. 2010. Development of monocytes, macrophages, and dendritic cells. *Science* 327:656-661.

Getts, D.R., R.L. Terry, M.T. Getts, M. Muller, S. Rana, B. Shrestha, J. Radford, N. Van Rooijen, I.L. Campbell, and N.J. King. 2008. Ly6c+ "inflammatory monocytes" are microglial precursors recruited in a pathogenic manner in West Nile virus encephalitis. *The Journal of experimental medicine* 205:2319-2337.

Gordon, S., and A. Pluddemann. 2019. The Mononuclear Phagocytic System. Generation of Diversity. *Frontiers in immunology* 10:1893.

Gordon, S.R., R.L. Maute, B.W. Dulken, G. Hutter, B.M. George, M.N. McCracken, R. Gupta, J.M. Tsai, R. Sinha, D. Corey, A.M. Ring, A.J. Connolly, and I.L. Weissman. 2017. PD-1 expression by tumour-associated macrophages inhibits phagocytosis and tumour immunity. *Nature* 545:495-499.

Gupta, S., A. Jain, S.N. Syed, R.G. Snodgrass, B. Pfluger-Muller, M.S. Leisegang, A. Weigert, R.P. Brandes, I. Ebersberger, B. Brune, and D. Namgaladze. 2018. IL-6 augments IL-4-induced polarization of primary human macrophages through synergy of STAT3, STAT6 and BATF transcription factors. *Oncoimmunology* 7:e1494110.

Hänzelmann, S., R. Castelo, and J. Guinney. 2013. GSVA: gene set variation analysis for microarray and RNA-seq data. *BMC bioinformatics* 14:7.

Hashimoto, D., A. Chow, C. Noizat, P. Teo, M.B. Beasley, M. Leboeuf, C.D. Becker, P. See, J. Price, D. Lucas, M. Greter, A. Mortha, S.W. Boyer, E.C. Forsberg, M. Tanaka, N. van Rooijen, A. Garcia-Sastre, E.R. Stanley, F. Ginhoux, P.S. Frenette, and M. Merad. 2013. Tissue-resident macrophages self-maintain locally throughout adult life with minimal contribution from circulating monocytes. *Immunity* 38:792-804.

Ho, I.-C., and S.-C. Miaw. 2016. Regulation of IL-4 Expression in Immunity and Diseases. In Regulation of Cytokine Gene Expression in Immunity and Diseases. X. Ma, editor Springer Netherlands, Dordrecht. 31-77.

Hoshino, A., B. Costa-Silva, T.L. Shen, G. Rodrigues, A. Hashimoto, M. Tesic Mark, H. Molina, S. Kohsaka, A. Di Giannatale, S. Ceder, S. Singh, C. Williams, N. Soplop, K. Uryu, L. Pharmer, T. King, L. Bojmar, A.E. Davies, Y. Ararso, T. Zhang, H. Zhang, J. Hernandez, J.M. Weiss, V.D. Dumont-Cole, K. Kramer, L.H. Wexler, A. Narendran, G.K. Schwartz, J.H. Healey, P. Sandstrom, K.J. Labori, E.H. Kure, P.M. Grandgenett, M.A. Hollingsworth, M. de Sousa, S. Kaur, M. Jain, K. Mallya, S.K. Batra, W.R. Jarnagin, M.S. Brady, O. Fodstad, V. Muller, K. Pantel, A.J. Minn, M.J. Bissell, B.A. Garcia, Y. Kang, V.K. Rajasekhar, C.M. Ghajar, I. Matei, H. Peinado, J. Bromberg, and D. Lyden. 2015. Tumour exosome integrins determine organotropic metastasis. *Nature* 527:329-335.

Jacome-Galarza, C.E., G.I. Percin, J.T. Muller, E. Mass, T. Lazarov, J. Eitler, M. Rauner, V.K. Yadav, L. Crozet, M. Bohm, P.L. Loyher, G. Karsenty, C. Waskow, and F. Geissmann. 2019. Developmental origin, functional maintenance and genetic rescue of osteoclasts. *Nature*

Kang, Y., P.M. Siegel, W. Shu, M. Drobnjak, S.M. Kakonen, C. Cordón-Cardo, T.A. Guise, and J. Massagué. 2003. A multigenic program mediating breast cancer metastasis to bone. *Cancer cell* 3:537-549.

Kitamura, T., B.Z. Qian, and J.W. Pollard. 2015a. Immune cell promotion of metastasis. *Nature reviews. Immunology* 15:73-86.

Kitamura, T., B.Z. Qian, D. Soong, L. Cassetta, R. Noy, G. Sugano, Y. Kato, J. Li, and J.W. Pollard. 2015b. CCL2-induced chemokine cascade promotes breast cancer metastasis by enhancing retention of metastasis-associated macrophages. *The Journal of experimental medicine* 212:1043-1059.

Li, X., W. Yao, Y. Yuan, P. Chen, B. Li, J. Li, R. Chu, H. Song, D. Xie, X. Jiang, and H. Wang. 2017. Targeting of tumour-infiltrating macrophages via CCL2/CCR2 signalling as a therapeutic strategy against hepatocellular carcinoma. *Gut* 66:157-167.

Li, Z., L. Chen, and Z. Qin. 2009. Paradoxical roles of IL-4 in tumor immunity. *Cellular & molecular immunology* 6:415-422.

Lin, E.Y., A.V. Nguyen, R.G. Russell, and J.W. Pollard. 2001. Colony-stimulating factor 1 promotes progression of mammary tumors to malignancy. *The Journal of experimental medicine* 193:727-740.

Liu, H., J. He, S.P. Koh, Y. Zhong, Z. Liu, Z. Wang, Y. Zhang, Z. Li, B.T. Tam, P. Lin, M. Xiao, K.H. Young, B. Amini, M.W. Starbuck, H.C. Lee, N.M. Navone, R.E. Davis, Q. Tong, P.L. Bergsagel, J. Hou, Q. Yi, R.Z. Orlowski, R.F. Gagel, and J. Yang. 2019. Reprogrammed marrow adipocytes contribute to myeloma-induced bone disease. *Science translational medicine* 11:

Maurizi, A., and N. Rucci. 2018. The Osteoclast in Bone Metastasis: Player and Target. *Cancers* 10:

Mohrs, M., B. Ledermann, G. Köhler, A. Dorfmüller, A. Gessner, and F. Brombacher. 1999. Differences between IL-4-and IL-4 receptor α-deficient mice in chronic leishmaniasis reveal a protective role for IL-13 receptor signaling. *The Journal of Immunology* 162:7302-7308.

Mundy, G.R. 2002. Metastasis to bone: causes, consequences and therapeutic opportunities. *Nature reviews. Cancer* 2:584-593.

Ojalvo, L.S., W. King, D. Cox, and J.W. Pollard. 2009. High-density gene expression analysis of tumor-associated macrophages from mouse mammary tumors. *The American journal of pathology* 174:1048-1064.

Palazon, A., P.A. Tyrakis, D. Macias, P. Velica, H. Rundqvist, S. Fitzpatrick, N. Vojnovic, A.T. Phan, N. Loman, I. Hedenfalk, T. Hatschek, J. Lovrot, T. Foukakis, A.W. Goldrath, J. Bergh, and R.S. Johnson. 2017. An HIF-1alpha/VEGF-A Axis in Cytotoxic T Cells Regulates Tumor Progression. *Cancer cell* 32:669-683 e665.

Palframan, R.T., S. Jung, G. Cheng, W. Weninger, Y. Luo, M. Dorf, D.R. Littman, B.J. Rollins, H. Zweerink, A. Rot, and U.H. von Andrian. 2001. Inflammatory Chemokine Transport and Presentation in HEV. *The Journal of experimental medicine* 194:1361-1374.

Pearce, D.A., A.J. Nirmal, T.C. Freeman, and A.H. Sims. 2018. Continuous Biomarker Assessment by Exhaustive

Survival Analysis. *BioRxiv*

Perdiguero, E.G., and F. Geissmann. 2016. The development and maintenance of resident macrophages. *Nature immunology* 17:2-8.

Price, T.T., M.L. Burness, A. Sivan, M.J. Warner, R. Cheng, C.H. Lee, L. Olivere, K. Comatas, J. Magnani, H. Kim Lyerly, Q. Cheng, C.M. McCall, and D.A. Sipkins. 2016. Dormant breast cancer micrometastases reside in specific bone marrow niches that regulate their transit to and from bone. *Science translational medicine* 8:340ra373.

Prost, S., R.E. Kishen, D.C. Kluth, and C.O. Bellamy. 2016. Working with Commercially Available Quantum Dots for Immunofluorescence on Tissue Sections. *PloS one* 11:e0163856.

Pyonteck, S.M., L. Akkari, A.J. Schuhmacher, R.L. Bowman, L. Sevenich, D.F. Quail, O.C. Olson, M.L. Quick, J.T. Huse, V. Teijeiro, M. Setty, C.S. Leslie, Y. Oei, A. Pedraza, J. Zhang, C.W. Brennan, J.C. Sutton, E.C. Holland, D. Daniel, and J.A. Joyce. 2013. CSF-1R inhibition alters macrophage polarization and blocks glioma progression. *Nature medicine* 19:1264-1272.

Qian, B., Y. Deng, J.H. Im, R.J. Muschel, Y. Zou, J. Li, R.A. Lang, and J.W. Pollard. 2009. A distinct macrophage population mediates metastatic breast cancer cell extravasation, establishment and growth. *PloS one* 4:e6562.

Qian, B.Z., J. Li, H. Zhang, T. Kitamura, J. Zhang, L.R. Campion, E.A. Kaiser, L.A. Snyder, and J.W. Pollard. 2011. CCL2 recruits inflammatory monocytes to facilitate breast-tumour metastasis. *Nature* 475:222-225.

Qian, B.Z., and J.W. Pollard. 2010. Macrophage diversity enhances tumor progression and metastasis. *Cell* 141:39-51.

Quail, D.F., and J.A. Joyce. 2016. Molecular Pathways: Deciphering Mechanisms of Resistance to Macrophage-Targeted Therapies. *Clinical cancer research : an official journal of the American Association for Cancer Research*

Ritchie, M.E., B. Phipson, D. Wu, Y. Hu, C.W. Law, W. Shi, and G.K. Smyth. 2015. limma powers differential expression analyses for RNA-sequencing and microarray studies. *Nucleic Acids Res* 43:e47.

Ruffell, B., and L.M. Coussens. 2015. Macrophages and therapeutic resistance in cancer. *Cancer cell* 27:462-472.

Schulz, C., E. Gomez Perdiguero, L. Chorro, H. Szabo-Rogers, N. Cagnard, K. Kierdorf, M. Prinz, B. Wu, S.E. Jacobsen, J.W. Pollard, J. Frampton, K.J. Liu, and F. Geissmann. 2012. A lineage of myeloid cells independent of Myb and hematopoietic stem cells. *Science* 336:86-90.

Sethi, N., X. Dai, C.G. Winter, and Y. Kang. 2011. Tumor-derived JAGGED1 promotes osteolytic bone metastasis of breast cancer by engaging notch signaling in bone cells. *Cancer cell* 19:192-205.

Shi, C., T. Jia, S. Mendez-Ferrer, T.M. Hohl, N.V. Serbina, L. Lipuma, I. Leiner, M.O. Li, P.S. Frenette, and E.G. Pamer. 2011. Bone marrow mesenchymal stem and progenitor cells induce monocyte emigration in response to circulating toll-like receptor ligands. *Immunity* 34:590-601.

Shiozawa, Y., E.A. Pedersen, A.M. Havens, Y. Jung, A. Mishra, J. Joseph, J.K. Kim, L.R. Patel, C. Ying, A.M. Ziegler, M.J. Pienta, J. Song, J. Wang, R.D. Loberg, P.H. Krebsbach, K.J. Pienta, and R.S. Taichman. 2011. Human prostate cancer metastases target the hematopoietic stem cell niche to establish footholds in mouse bone marrow. *The Journal of clinical investigation* 121:1298-1312.

Sierra-Filardi, E., C. Nieto, A. Dominguez-Soto, R. Barroso, P. Sanchez-Mateos, A. Puig-Kroger, M. Lopez-Bravo, J. Joven, C. Ardavin, J.L. Rodriguez-Fernandez, C. Sanchez-Torres, M. Mellado, and A.L. Corbi. 2014. CCL2 shapes macrophage polarization by GM-CSF and M-CSF: identification of CCL2/CCR2-dependent gene expression profile. *J Immunol* 192:3858-3867.

Stanley, E.R., K.L. Berg, D.B. Einstein, P.S. Lee, F.J. Pixley, Y. Wang, and Y.G. Yeung. 1997. Biology and action of colony‐stimulating factor‐1. *Molecular Reproduction and Development: Incorporating Gamete Research* 46:4-10.

Therneau, T.M., and P.M. Grambsch. 2000. Modeling survival data: extending the Cox model. Springer Science & Business Media,

Van Rooijen, N., and A. Sanders. 1994. Liposome mediated depletion of macrophages: mechanism of action, preparation of liposomes and applications. *Journal of immunological methods* 174:83-93.

Varin, A., S. Mukhopadhyay, G. Herbein, and S. Gordon. 2010. Alternative activation of macrophages by IL-4 impairs phagocytosis of pathogens but potentiates microbial-induced signalling and cytokine secretion. *Blood* 115:353-362.

Venmar, K.T., K.J. Carter, D.G. Hwang, E.A. Dozier, and B. Fingleton. 2014. IL4 receptor ILR4alpha regulates metastatic colonization by mammary tumors through multiple signaling pathways. *Cancer Res* 74:4329-4340.

Wang, H., C. Yu, X. Gao, T. Welte, A.M. Muscarella, L. Tian, H. Zhao, Z. Zhao, S. Du, J. Tao, B. Lee, T.F. Westbrook,

S.T. Wong, X. Jin, J.M. Rosen, C.K. Osborne, and X.H. Zhang. 2015. The osteogenic niche promotes early-stage bone colonization of disseminated breast cancer cells. *Cancer cell* 27:193-210.

Weilbaecher, K.N., T.A. Guise, and L.K. McCauley. 2011. Cancer to bone: a fatal attraction. *Nature reviews. Cancer* 11:411-425.

Wu, J.B., L. Yin, C. Shi, Q. Li, P. Duan, J.M. Huang, C. Liu, F. Wang, M. Lewis, Y. Wang, T.P. Lin, C.C. Pan, E.M. Posadas, H.E. Zhau, and L.W. Chung. 2017. MAOA-Dependent Activation of Shh-IL6-RANKL Signaling Network Promotes Prostate Cancer Metastasis by Engaging Tumor-Stromal Cell Interactions. *Cancer cell* 31:368-382.

Wynn, T.A., A. Chawla, and J.W. Pollard. 2013. Macrophage biology in development, homeostasis and disease. *Nature* 496:445-455.

Xu, R., Y. Li, H. Yan, E. Zhang, X. Huang, Q. Chen, J. Chen, J. Qu, Y. Liu, J. He, Q. Yi, and Z. Cai. 2019. CCL2 promotes macrophages-associated chemoresistance via MCPIP1 dual catalytic activities in multiple myeloma. *Cell Death Dis* 10:781.

Yanagihara, Y., K. Ikizawa, K. Kajiwara, T. Koshio, Y. Basaki, and K. Akiyama. 1995. Functional significance of IL-4 receptor on B cells in IL-4-induced human IgE production. *Journal of Allergy and Clinical Immunology* 96:1145-1151.

Yang, M., D. McKay, J.W. Pollard, and C.E. Lewis. 2018. Diverse Functions of Macrophages in Different Tumor Microenvironments. *Cancer Res* 78:5492-5503.

Zhang, X.H., Q. Wang, W. Gerald, C.A. Hudis, L. Norton, M. Smid, J.A. Foekens, and J. Massague. 2009. Latent bone metastasis in breast cancer tied to Src-dependent survival signals. *Cancer cell* 16:67-78.

Zhu, Y., J.M. Herndon, D.K. Sojka, K.W. Kim, B.L. Knolhoff, C. Zuo, D.R. Cullinan, J. Luo, A.R. Bearden, K.J. Lavine, W.M. Yokoyama, W.G. Hawkins, R.C. Fields, G.J. Randolph, and D.G. DeNardo. 2017. Tissue-Resident Macrophages in Pancreatic Ductal Adenocarcinoma Originate from Embryonic Hematopoiesis and Promote Tumor Progression. *Immunity* 47:323-338 e326.

Figure legends

Figure 1 MAMs depletion enhance the survival of mice with breast cancer bone metastasis

A) Representative immunofluorescent staining of CD68+ macrophages (Red) infiltrated in PanCK+ tumour area (Green) of breast cancer bone metastasis patient sample. Nuclei were stained with Qred. Bar equals 20µm.
B) Representative immunofluorescent staining of Iba1+ macrophages (Red) in bone metastasis of 1833 human breast cancer cells (left) and MetBo2 murine breast cancer cells (right). Bar equals 20µm. Nuclei were stained with DAPI (Blue).
C) Diagram of macrophage depletion in established bone metastasis detected by bioluminescent (BLI) imaging with various treatment until humane endpoint.
D) Representative images and quantification of bioluminescent signal of MetBo2 bone metastasis treated with Liposome clodronate (L-Clod) or corresponding vehicle (L-PBS). Signals were quantified by PhotonIMAGER and are normalized to day 0. Bar represent SEM, N=6-8 mice for each group. ** P<0.01 with student t test. Experiments performed 3 times independently.
E) Representative figures and quantification of bioluminescent signal of MetBo2 bone metastasis treated with BLZ945 (BLZ) or corresponding vehicle (Veh). Signals were quantified by PhotonIMAGER and normalized to day 0. Bar represent SEM, N=6-8 mice for each group. ***, P<0.001 with student t test. Experiments performed 3 times independently.
F) Representative figures and quantification of bioluminescent signal of 1833 bone metastasis treated with BLZ945 (BLZ) or corresponding vehicle (Veh). Signals were quantified by PhotonIMAGER and normalized to day 0. Bar represent SEM, N=6-8 mice for each group. ***, P<0.001 with student t test. Experiments performed 2 times independently.

Figure 2 CCL2 recruited inflammatory monocyte promote bone metastasis growth

A) Diagram of adoptive transfer of monocytes in healthy mice and mice with bone metastasis. i.v., intravenous.
B) Relative number of recruited inflammatory monocytes (IM) and patrolling monocytes (PM) in bone of recipient mice bearing bone metastasis or healthy control. N= 6, *, P<0.05 with student t test
C) Survival curve of mice with MetBo2 bone metastasis (death defined as time taken to reach the humane end point). WT n=4; KO n=9 p =0.0133
D) Representative images and quantification of bioluminescent signal for MetBo2 murine bone metastasis in *Ccr2*-/- mice and wild type mice. Signals were quantified by PhotonIMAGER and normalized to day 0. CCR2-/- group n=8 mice, wild-type group n=7 mice. Bar represent SEM. **, P<0.01 with student t test. Experiments performed 4 times independently.
E) Survival curve of mice with bone metastasis. Death is defined as time the mice take to reach the humane clinical end point. P=0.0332
F) Representative images and quantification of bioluminescent signal for 1833 human bone metastasis model in *Ccr2* -/- mice and wild type mice. Signals were measured by IVIS and normalized to day 0. $CCR2^{-/-}$group n=8 mice, control group n=7 mice. Bar represent SEM. ***, P<0.001 with student t test
G) Quantification of bioluminescent signal for 1833 human bone metastasis model treated with CCL2 inhibitor or corresponding vehicle (control). Signals were measured by IVIS and normalized to day 0. CCL2 antibody treated group n=8 mice, control group n=7 mice. Bar represent SEM. ***, P<0.001 with student t test
H) Diagram and quantification of bioluminescent signal for transferring monocytes. Recipient mice are CCR2-deficient mice with 1833 bone metastasis. Monocytes from wild-type mice and CCR2-deficient mice were injected intravenously after tumour signal detected. Bioluminescent signal on the legs were quantified by PhotonIMAGER and signals are normalized to day 0. Each group contain data from 4 legs. Bar represent SEM. ***, P<0.001 with student t test.

Experiments performed 3 times independently.

Figure 3 Bone metastasis associated macrophages bear distinct cell surface markers

A) Pie chart of the total number of differentially expressed genes that are upregulated or downregulated in macrophages associated with bone metastasis compare with macrophages from normal bone. Differentially expressed genes are defined as fold change >1.5, p<0.01.
B) Heatmap showing the expression of major macrophage polarization markers. Bar denote the relative expression level of each gene in each sample.
C) Heatmap showing the expression of genes of major tumour promoting functions. Bar denote the relative expression level of each gene in each sample. Representative histogram of different macrophage markers in bone marrow macrophages from healthy mice (blue), bone metastasis (red) and adjacent normal (peri-tumour) (green). Grey represents isotype control. Experiments performed 3 times independently.
D) Representative histogram of different macrophage markers in bone marrow macrophages from healthy mice (blue), bone metastasis (red) and adjacent normal (peri-tumour) (green). Grey represents isotype control. Experiments performed 3 times independently.
E) Representative flow dot plot of CD204 and IL-4R(CD124) expression in macrophages from healthy bone marrow and bone metastasis associated macrophages. Experiments performed 3 times independently.
F) Representative immunofluorescent staining of CD204 and F4/80 in MetBo2 bone metastasis and adjacent normal bone marrow. Bar equals 50μm. T denotes tumour area. Experiments performed 3 times independently.
G) Representative immunofluorescent staining of CD204+ macrophage populations co-expressing Iba-1 and IL-4R in bone metastasis. Bar equals 20μm. Arrows point out the co-expression of markers (yellow) on macrophages. Experiments performed 3 times independently.

Figure 4 Bone metastasis associated macrophages in human samples

A) Multiplex immunofluorescent staining of CD204 and IL4R macrophage in patient breast cancer bone metastasis (Bar equals 20μm) and quantification (N=9 samples, Bar represent SEM).
B) IL4 target score correlation with CD204 expression in patient bone metastasis transcriptome datasets. Kaplan-Meyer curve showing survival probability in breast cancer patients classified based on upper quantile expression of IL4R (n=113). Significance and HR values were calculated for all possible separation points (cut-off) using *survivALL* package in R. Heatmap on the left shows range of IL4R expression in samples and significant (P<0.05, HR>1) cut-offs (gray).

Figure 5 Monocyte derived macrophage promotion of bone metastasis is IL4R dependent

A) CD204 expression of CCR2+ and CCR2- monocytes from healthy control and bone metastasis. Grey: isotype control. Red: CCR2+ monocytes. Blue: CCR2- monocytes. N=3.
B) Volcano plot showing Il4ra highly upregulated in monocytes from MetBo2 bone metastases compared with monocytes sorted from healthy mice. Volcano plot showing -log10(p value) versus log2FC. Red coloured points represent upregulated gene with p<0.05 and fold change > 1.5; Green coloured points represent downregulated gene with p<0.05 and fold change > 1.5.
C) Diagram of GFP+ monocyte adoptive transfer into bone metastasis bearing syngeneic host (left) and (right) representative FACS histogram showing CD204 and IL4R expression comparing monocyte derived macrophages (GFP+) and endogenous macrophages (GFP-). Grey: isotype control. Red: GFP+ macrophages. Blue: GFP- macrophages. N=3.
D) Diagram of bone colonization assay in mosaic mice bearing *Il4r+/-* and *Il4r-/-* bone marrow (left). Representative images and quantification of bioluminescent signal of 1833 bone metastasis in bone marrow (BM) mosaic mice generated as described in the diagram (right). Signals were measured by IVIS and normalized to day 0. n=10 for each group. Bar represent

SEM. ***p<0.001 with student t test. Experiments performed 2 times independently.

E) Representative images and quantification of bioluminescent signal of 1833 bone metastasis in mice adopted with wild-type or *Il4r*-/- monocytes. Signals were quantified by PhotonIMAGER and normalized to day 0. n=3-5. Bar represent SEM. Each group contain data from 4 legs. Bar represent SEM. ***, P<0.001 with student t test. Experiments performed 3 times independently.

Supplementary 1

A) FACS quantification of bone marrow immune cell populations from MetBo2 bone metastases treated with liposome clodronate (L-Clod), or control liposome (L-PBS). Bar represent SEM, N=3 mice for each group. * P<0.05 with student t test.

B) FACS quantification of bone marrow immune cell populations from MetBo2 bone metastases treated with CSF1R inhibitor BLZ and vehicle treatment. Bar represent SEM, N=3 mice for each group. * P<0.05 with student t test.

C) Quantification of bioluminescent signal in the abdomin of MetBo2 bone metastasis model treated with Liposome clodronate (L-Clod) or corresponding vehicle (L-PBS). Signals were quantified by PhotonIMAGER and normalized to day 0. Bar represent SEM. N equals the number of mice included in quantification.

D) Representative figures and quantification of bioluminescent signal in the abdomin of MetBo2 bone metastasis treated with BLZ945 (BLZ) or corresponding vehicle (Veh). Signals were quantified by PhotonIMAGER and normalized to day 0. Bar represent SEM. N equals the number of mice included in quantification. In mice with chest metastasis, only one mouse in vehicle group survived after 10 days.

Supplementary 2

A) Representative TRAP staining and quantification of MetBo2 bone metastasis. Sample treated with free clodronate, liposome clodronate or corresponding vehicles until end point. Bar equals 20µm.

B) Quantification of osteoclasts in bone metastasis. ***, P<0.001. N=5 for each group.

C) Quantification of macrophages in MetBo2 bone metastasis. Sample treated with free clodronate, liposome clodronate or corresponding vehicles until the clinical end point. N=3 for each group. *, P<0.05; **, P<0.01.

D) Representative figures and quantification of bioluminescent signal of bone metastasis treated with free clodronate (F-clod), Liposome clodronate (L-Clod) or corresponding vehicle (Veh) in MetBo2 murine breast cancer model. Signals were quantified by PhotonIMAGER and normalized to day 0. *, P<0.05, ***, P<0.001. N=6-8 mice for each group. Experiments performed 2 times independently.

Supplementary 3

A) Representative immunofluorescent staining showing that most of the CD169+ macrophages do not infiltrate in bone metastasis. Bar equals 50µm. T denotes tumour area. Green: CD169, Red: F4/80, Blue: DAPI

B) Representative FACS plot and quantification showing ablation of bone marrow macrophage (CD11b+F4/80+SSC^{low}, % of all immune cells) in mice treated with DT or control Glu-DT. Bar represent SEM, N=3 mice for each group. * P<0.05 with student t test.

C) Quantification of Bioluminescent signal of MetBo2 bone metastasis in CD169-DTR mice treated with DT or Glu-DT. Signals were quantified by PhotonIMAGER and normalized to day 0. Bar represent SEM, N=4-8 tumours for each group. Experiments repeated 2 times independently.

D) Representative immunofluorescent staining of MetBo2 bone metastasis in CD169-DTR mice showing depletion of CD169+ macrophages but not majority of Iba1+ macrophages in DT treated mice compared with control Glu-DT treatment. Bar equals 50µm. Red: CD169, blue:

DAPI.

Supplementary 4

A) Absolute number of inflammatory monocytes (IM) and patrolling monocytes (PM) in blood of CCR2 knockout mice and wild type mice. Bar represent SEM. N= 3 mice for each group, *, P<0.05 with student t test.
B) Absolute number of inflammatory monocytes (IM) and patrolling monocytes (PM) per leg in bone marrow of CCR2 knockout mice and wild type mice. Bar represent SEM. N= 3 mice for each group, *, P<0.05 with student t test.

Supplementary 5

A) Representative TRAP staining and quantification of 1833 bone metastasis from mosaic mice bearing *Il4r+/-* and *Il4r -/-* bone marrow. Bar equals 20µm. Bar represent SEM. N= 3 mice for each group.
B) Representative FACS plot and quantification showing monocytes and macrophage change in mosaic mice bearing *Il4r+/-* and *Il4r -/-* bone marrow. Bar represent SEM. N= 3 mice for each group, *, P<0.05 with student t test. Experiments performed 2 times independently.
C) Relative expression of IL-4 in different cell types in MetBo2 bone metastasis. Immune cell populations and tumour cells from bone metastasis enriched sample were sorted based on the lineage marker and RNA was extracted for qPCR quantification.

Supplementary Table 1. Clinical information for the breast cancer bone patients.

Figure 1 MAMs depletion enhance the survival of mice with breast cancer bone metastasis

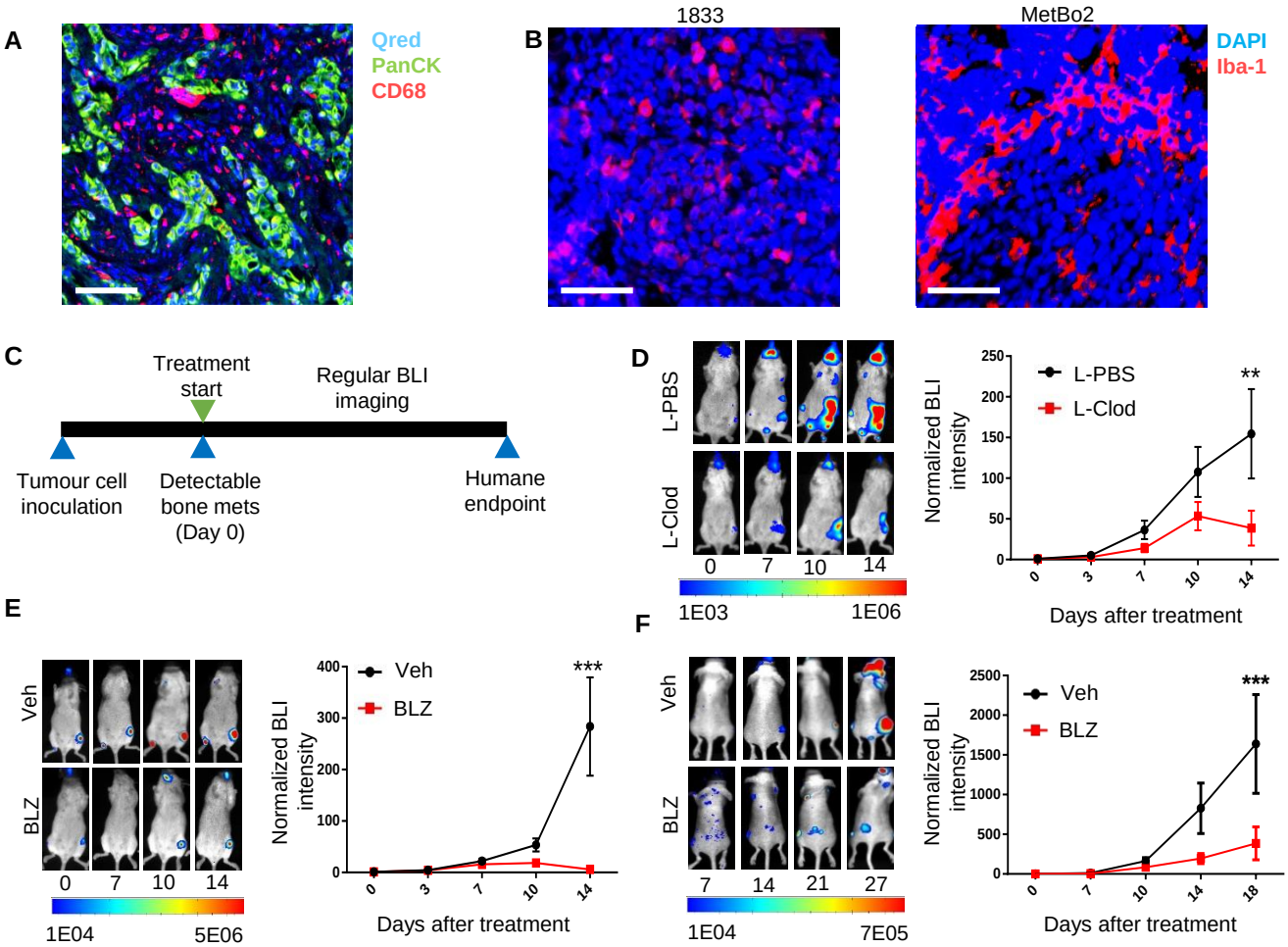

Figure 2 CCL2 recruited inflammatory monocytes promote bone metastasis growth

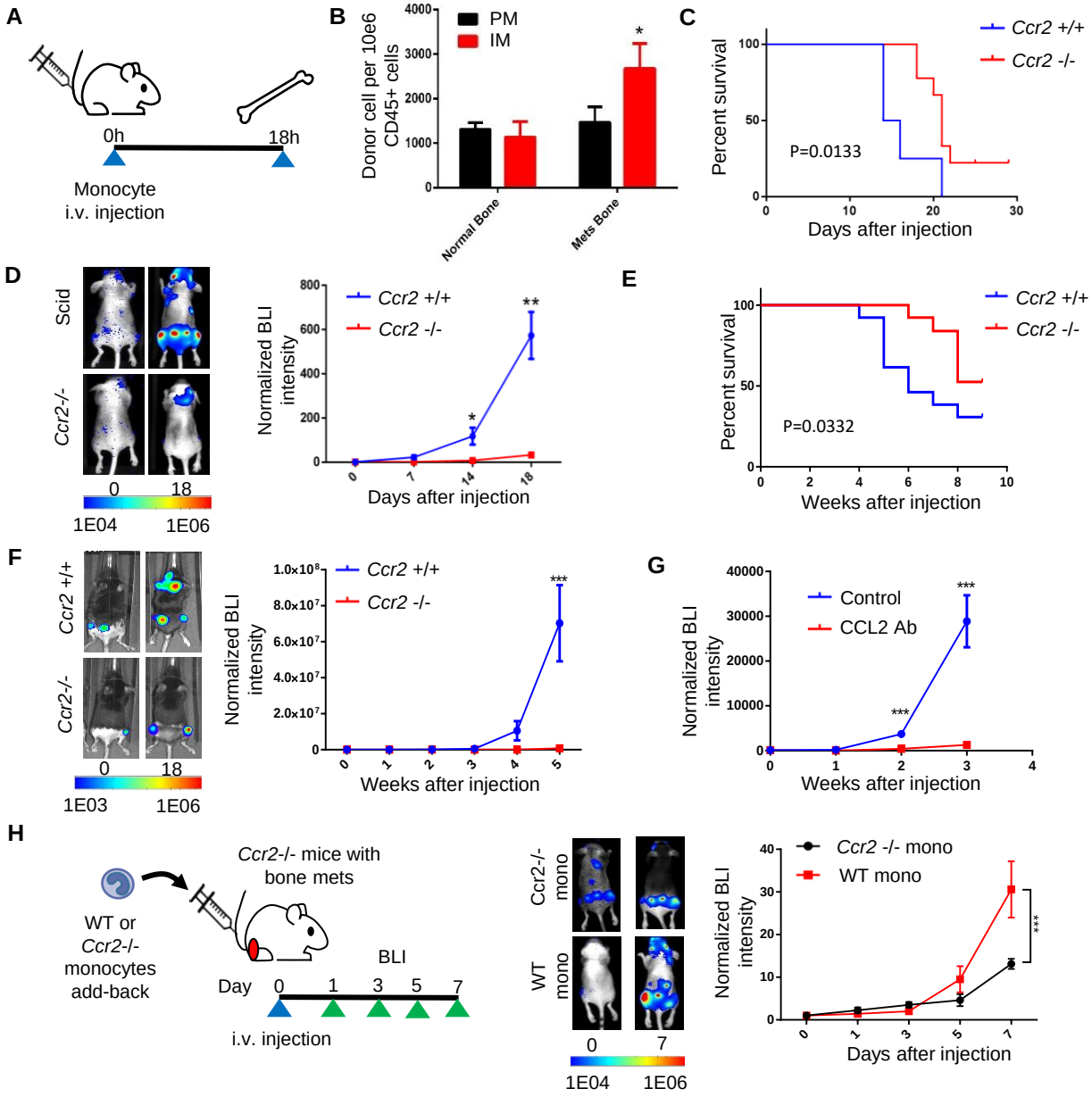

Figure 3 Bone metastasis associated macrophages bear distinct cell surface markers

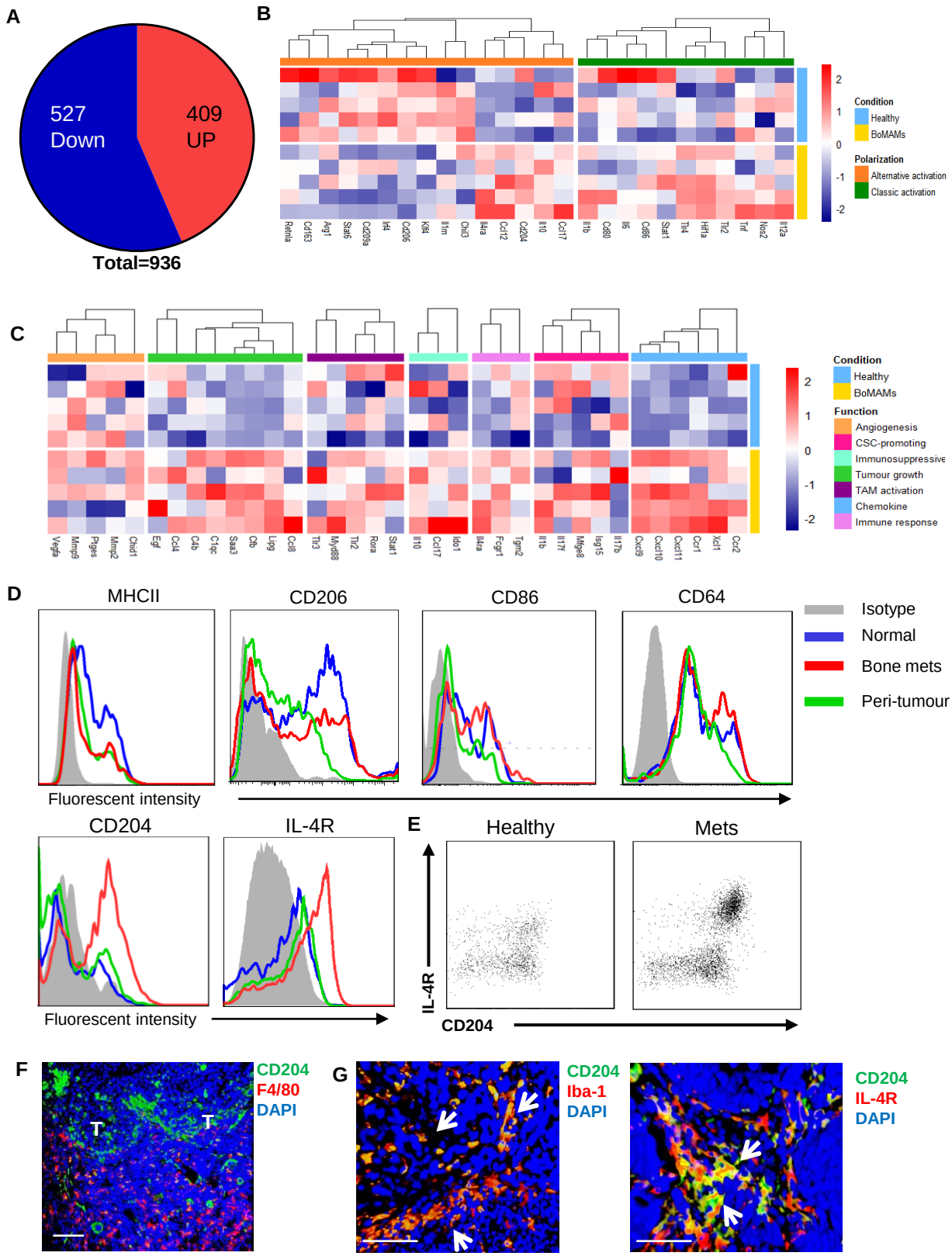

Figure 4 Bone metastasis associated macrophages in human sample

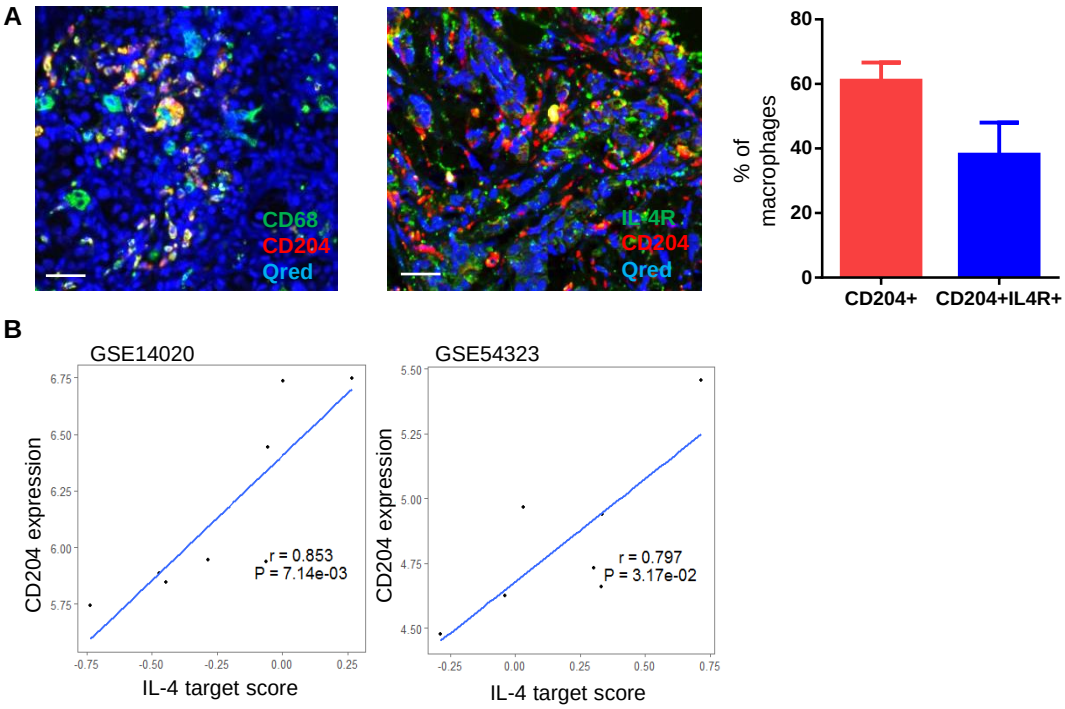

Figure 5 Monocyte derived macrophage promotion of bone metastasis is IL4R dependent

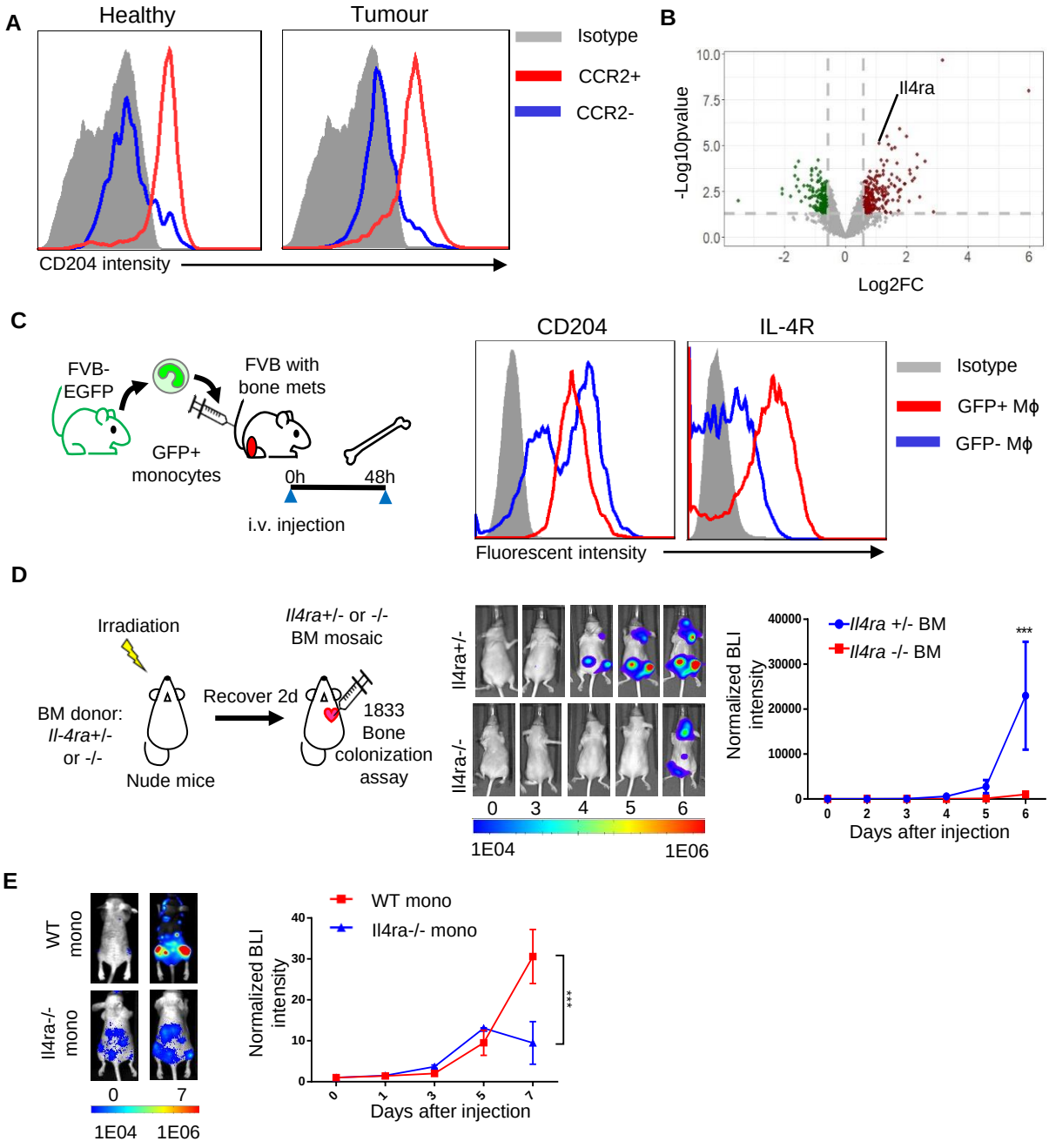

Supplementary 1

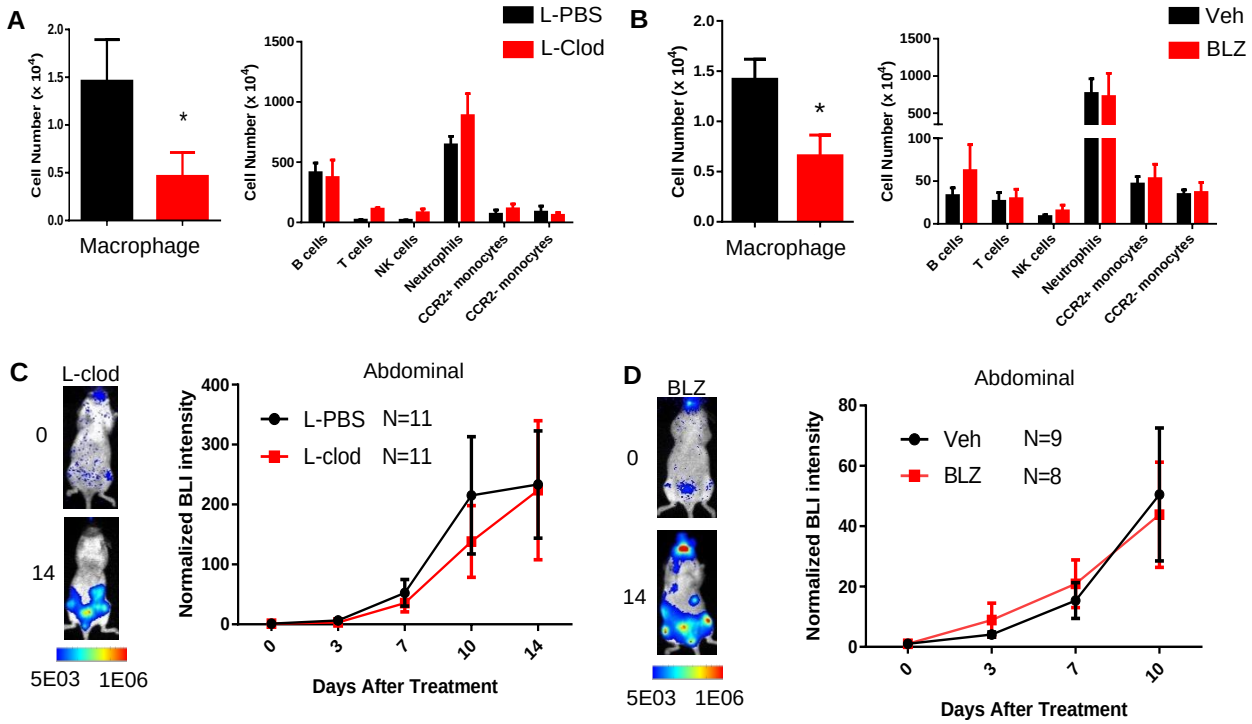

Supplementary 2

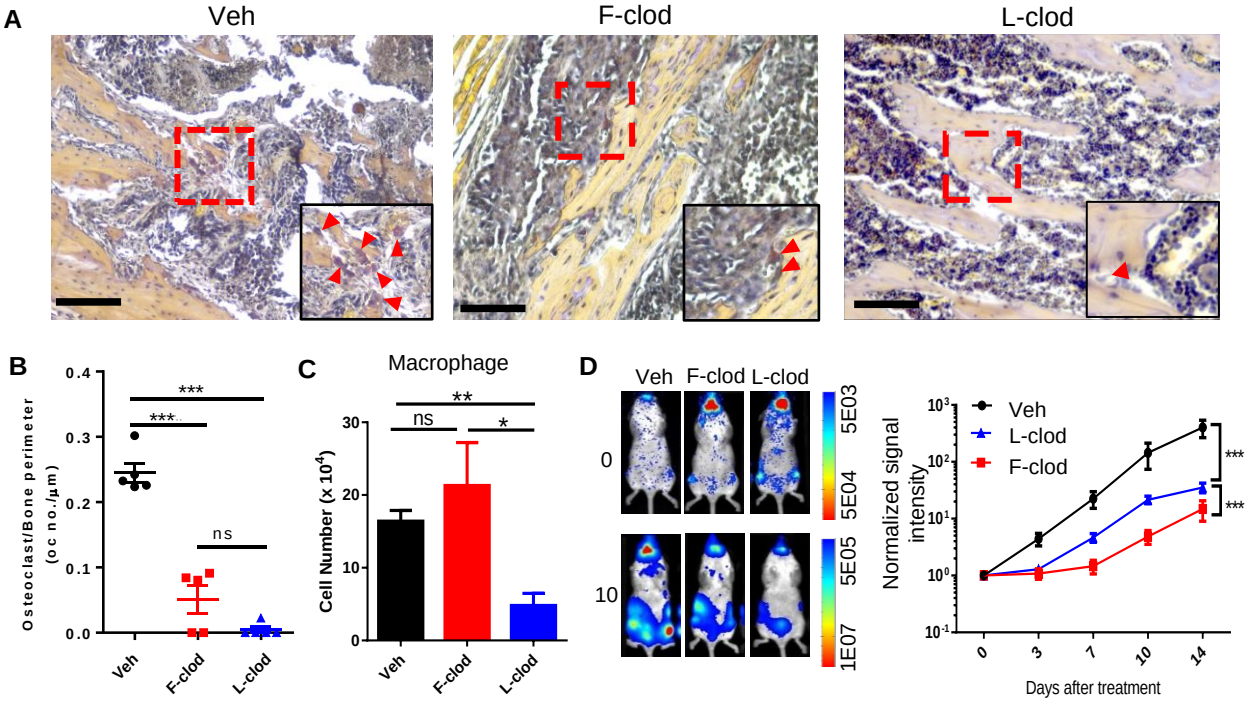

Supplementary 3

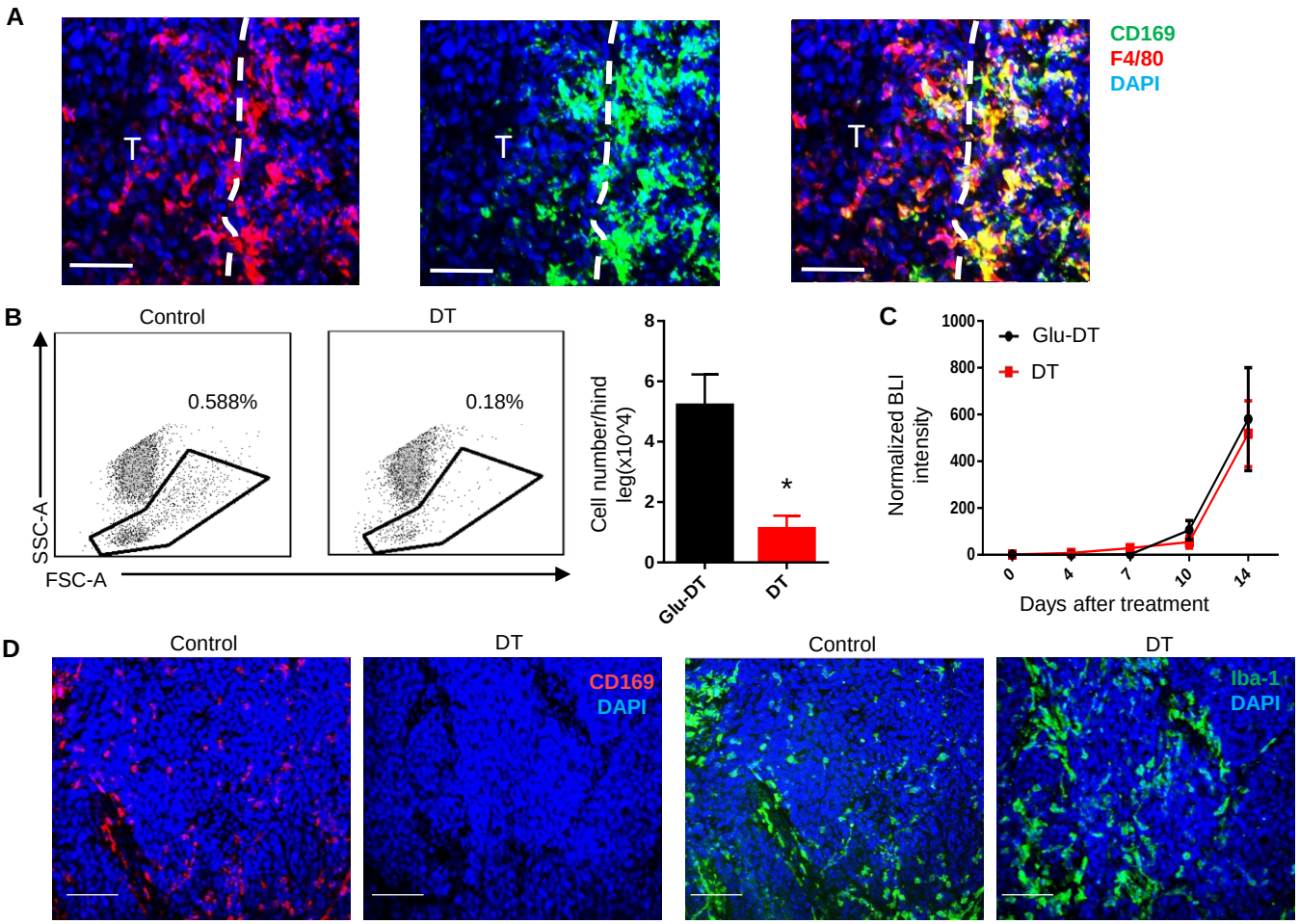

Supplementary 4

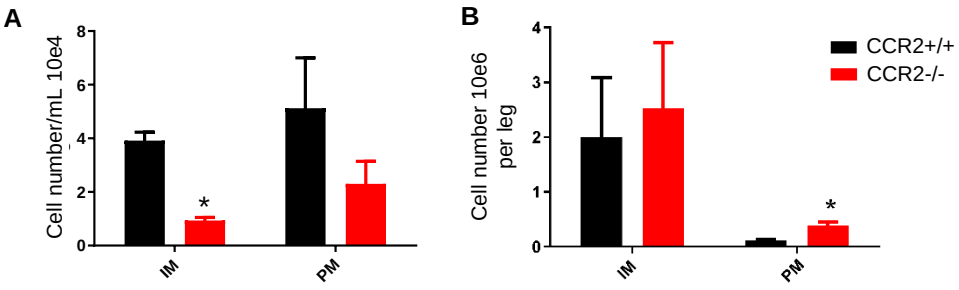

Supplementary 5

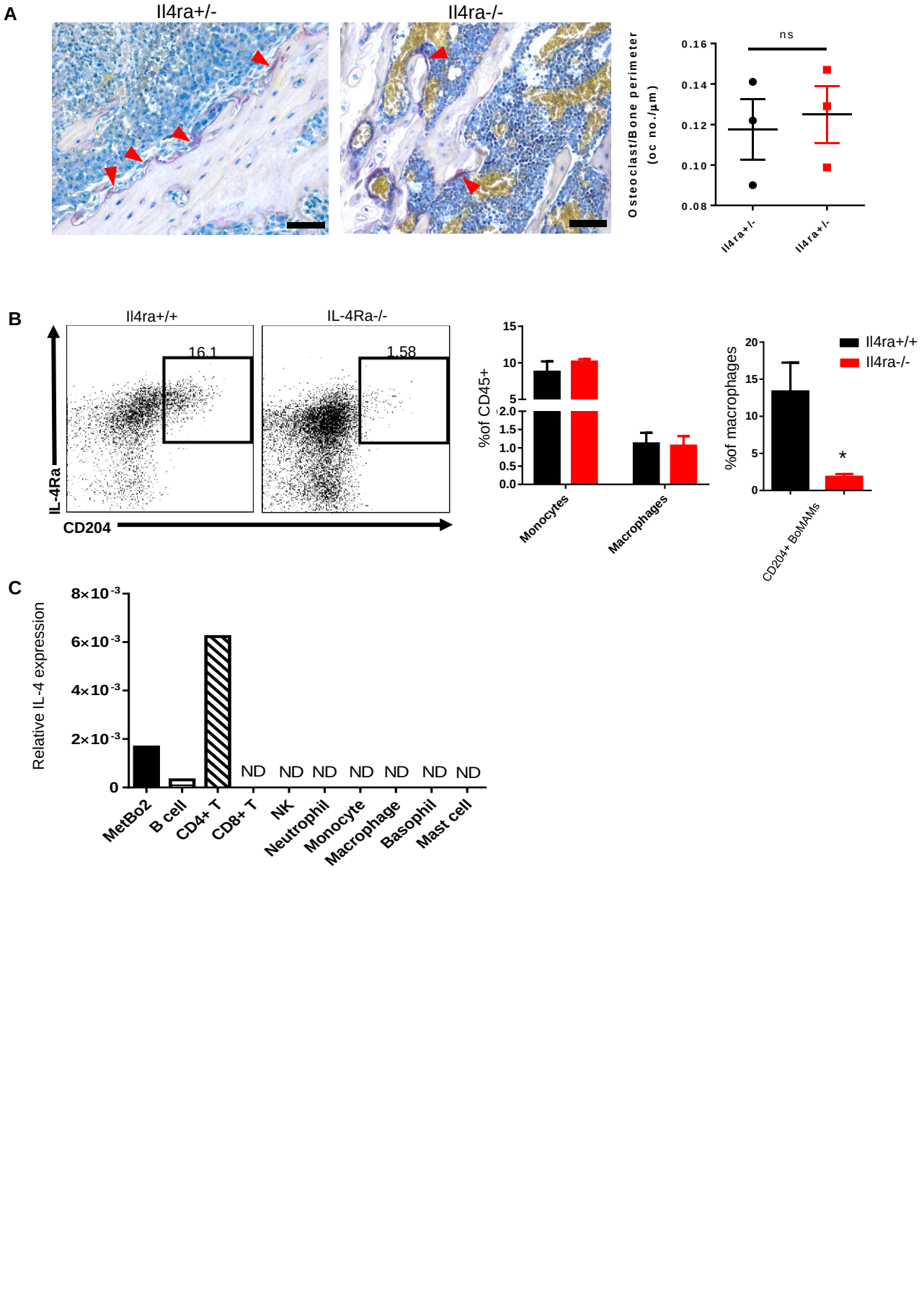

Supplementary table 1 Clinical information for the 9 bone metastasis samples from breast cancer patients

Code	Gender	Age	Cancer type	Site	ER	PR	HER-2(BC)
B16-9797	F	52	BCa	T7	1% +	-	2+
B16-13100	F	37	BCa	T7	70% +	40% +	2+
B16-13970	F	29	BCa	C7, T1	-	-	3+
B17-254	F	50	BCa	Femur	90%+	20%+	2+
B17-8203	F	48	BCa	Ilium	70%+	80% +	-
B17-9149	F	54	BCa	C4,T2	90%+	60%	-
B17-16751	F	54	BCa	Hip	80% +	90% +	2+
B17-19574	F	50	BCa	Acetabular	100% +	95% +	0
B17-24877	F	50	BCa	Humerus	>95% 3+	-	0-1 +